

Maximum A Posteriori Direction-of-Arrival Estimation via Mixed-Integer Semidefinite Programming

Tianyi Liu^{1b}, Frederic Matter^{1b}, Alexander Sorg, Marc E. Pfetsch^{1b}, Martin Haardt^{1b}, and Marius Pesavento^{1b}

Abstract—In this paper, we consider the maximum a posteriori (MAP) estimation for the multiple measurement vectors (MMV) problem with application to direction-of-arrival (DOA) estimation, which is classically formulated as a regularized least-squares (LS) problem with an $\ell_{2,0}$ -norm constraint, and derive an equivalent mixed-integer semidefinite program (MISDP) reformulation. The proposed MISDP reformulation can be exactly solved by a generic MISDP solver using a semidefinite programming (SDP) based branch-and-bound method, which, unlike other nonconvex approaches for the MMV problem, such as the greedy methods and sparse Bayesian learning techniques, provides a solution with an optimality assessment even with early termination. We also present an approximate solution approach based on randomized rounding that yields high-quality feasible solutions of the proposed MISDP reformulation at a practically affordable computation time for problems of extremely large dimensions. Numerical simulations demonstrate the improved error performance of our proposed method in comparison to several popular DOA estimation methods. In particular, compared to the deterministic maximum likelihood (DML) estimator, which is often used as a benchmark, the proposed method applied with the randomized rounding algorithm exhibits a superior estimation performance at a significantly reduced running time.

Index Terms—DOA estimation, multiple measurement vectors, joint sparsity, cardinality constraint, $\ell_{2,0}$ -mixed-norm constraint, mixed-integer semidefinite program, maximum a posteriori estimation, randomized rounding

I. INTRODUCTION

THE multiple measurement vectors (MMV) problem is a fundamental challenge in signal processing and compressed sensing. It involves the joint estimation of multiple signals that share a common sparse support over a known dictionary. The MMV problem arises in various applications, e.g., imaging [1], communications [2], [3], and signal processing [4]. The MMV problem is also known by several other names in the literature, e.g., simultaneous sparse coding [5],

joint sparse coding [6], and simultaneous sparse approximation [7], [8].

Similar to the classical sparse signal reconstruction from a single measurement vector (SMV), the MMV problem is NP-hard due to the combinatorial nature of the cardinality constraint [9], [10]. Hence, approximate procedures are conventionally applied. Many existing approximate solution approaches for the SMV case have been extended to the MMV case. Those approaches can be roughly divided into greedy methods [3], [7], [11], [12], convex relaxation approaches based on minimization of diversity measures [3], [8], [13]–[15], and sparse Bayesian learning methods [16], [17]. The diversity minimization methods achieve sparse solutions by introducing in the objective function a penalty, referred to as the diversity measure, that is computationally convenient and encourages joint sparsity. In particular, as a natural extension of basis pursuit [18] or LASSO [19] for the SMV case, the $\ell_{2,1}$ -mixed-norm penalty is investigated in [3], [13]. An equivalent compact reformulation of the $\ell_{2,1}$ -mixed-norm minimization, named SPARROW, is proposed in [14], which can be solved at a significantly reduced running time. The diversity minimization methods belong to the category of regularization-based methods, which can be equivalently interpreted as maximum a posteriori (MAP) estimators with different priors under the framework of Bayesian inference [20]. Another class of methods established in the Bayesian framework is known as sparse Bayesian learning (SBL). In contrast to the diversity minimization methods, where the parameters of the prior distribution are assumed to be known and considered as tuning parameters, in the sparse Bayesian learning framework, the prior parameters are estimated by a type-II maximum likelihood, i.e., by maximizing the marginal likelihood that has been integrated over the parameter space [16]. Although this marginal likelihood is multimodal, various iterative algorithms have been employed to efficiently obtain its stationary points, including the EM algorithm and other fixed-point methods [16], [17]. Recovery guarantees of several aforementioned methods for the MMV problem are established in [12], [21]–[25].

MMV-based parameter estimation is a classical problem in various applications in array signal processing including direction-of-arrival (DOA) estimation [26]–[30]. As a prominent class of DOA estimation methods, the subspace-based methods have been developed by exploiting the eigenstructure of the spatial correlation matrix, including the Multiple Signal Classification (MUSIC) and ESPRIT along with their

This work was supported in part by the DFG PRIDE Project PE 2080/2-1 and in part by the EXPRESS II Project within the DFG priority program CoSIP (DFG-SPP 1798).

Tianyi Liu, Alexander Sorg, and Marius Pesavento are with the Communications Systems Group, Technical University of Darmstadt, 64283 Darmstadt, Germany (e-mail: tliu@nt.tu-darmstadt.de; alex@mail.ramanujan.eu; pesavento@nt.tu-darmstadt.de).

Frederic Matter and Marc E. Pfetsch are with the Research Group Optimization, Technical University of Darmstadt, 64283 Darmstadt, Germany (e-mail: frederic.matter@gmx.de; pfetsch@mathematik.tu-darmstadt.de).

Martin Haardt is with the Communications Research Laboratory, Ilmenau University of Technology, 98684 Ilmenau, Germany (e-mail: martin.haardt@tu-ilmenau.de).

Part of this work is accepted for publication at IEEE CAMSAP 2023.

variants [31]–[34]. However, in the case of correlated source signals and/or low sample sizes, the classical subspace-based methods experience a dramatic performance degradation as the signal subspace becomes rank deficient. A common alternative approach that is known to be robust to the signal correlation is the deterministic maximum likelihood (DML) estimation, which is formulated as a nonlinear least-squares (LS) problem. The DML estimation has remarkable error performance in both the threshold and asymptotic region by fully exploiting the data model. Nevertheless, due to the nonlinearity and multimodality, the DML estimation is computationally expensive and generally requires a multidimensional grid search to obtain the exact solution. Inspired by the capacity of compressed sensing [35], sparsity-based DOA estimation methods have been developed, where the DOA estimation from multiple snapshots is modeled as an MMV problem by introducing a predefined dictionary that is obtained from sampling the complete field-of-view (FOV) [30], [36]. The sparsity-based approach often exhibits excellent estimation performance in several demanding scenarios, including cases with a limited number of snapshots and highly correlated sources, at an affordable running time by using the aforementioned efficient methods for the MMV problem, such as the mixed-norm minimization [13], [14] and sparse Bayesian learning [17], [37], [38]. A comprehensive review of the sparsity-based methods for DOA estimation can be found in [36]. However, the relaxation of the cardinality measure in the mixed-norm minimization often leads to a degradation of the estimation quality and an asymptotic bias. On the other hand, although the SBL method provides more flexibility and avoids the overhead of tuning regularization parameters, its performance degrades dramatically in the cases with a large number of sources or high source correlations, as shown in the simulations in Section VIII.

In this paper, we consider the MAP estimation with an uncorrelated Gaussian prior for joint sparse signal reconstruction from multiple measurement vectors, with application to DOA estimation. In contrast to the mixed-norm minimization approaches, we employ the exact $\ell_{2,0}$ -norm constraint to avoid performance degradation caused by the relaxation of the cardinality constraint. The corresponding MAP estimator is formulated as a regularized LS problem with an $\ell_{2,0}$ -norm constraint, which can be viewed as a generalization of the ℓ_0 -norm constrained LS problem investigated in [39] from a single measurement to MMV case. In particular, compared to the DML, the uncorrelated Gaussian prior introduces an additional Tikhonov regularization into the MAP estimation problem, which can then be exactly reformulated as a mixed-integer semidefinite program (MISDP) by using the reformulation techniques in [39]. The presented MISDP reformulation can be viewed as an extension of the reformulation in [39] to the MMV case. However, we provide a different interpretation of the reformulation. The motivation for using the MAP estimator is that the MISDP problem class has recently been comprehensively studied in mathematical optimization. There exist several general-purpose solvers based on the state-of-the-art branch-and-bound method, such as SCIP-SDP [40]–[42], that can be employed to obtain a global optimum of

a MISDP problem more efficiently than the DML approach, which generally requires exhaustive search. Moreover, if the branch-and-bound solver is terminated early, an optimality assessment of the obtained solution is provided by the gap between the lower and upper bounds of the optimal value. Due to the incorporation of a randomized rounding procedure in the branch-and-bound approach, the SCIP-SDP solver often quickly finds an optimal or nearly optimal solution, but the verification of the optimality of the obtained solution may still be computationally expensive for problems of extremely large dimensions. Motivated by the above observation, we devise a randomized rounding algorithm, as an extension of the solution approach of Pilanci et al. in [39] for the single measurement case to the multiple measurement problem under consideration in order to obtain a satisfactory approximate solution at a significantly reduced computation time for large problem dimensions. Simulation results demonstrate the improved error performance of our proposed methods in comparison to several widely used DOA estimation methods. In particular, compared to the DML estimator obtained by brute-force search over a multidimensional grid, which is often used as a benchmark, the proposed MISDP-based method applied with the randomized rounding algorithm exhibits a superior error performance at a considerably reduced running time in difficult scenarios, e.g., in the case with a limited number of snapshots. Moreover, in contrast to other nonconvex approaches, including the greedy methods and the SBL method, the proposed MISDP-based method offers a guarantee of finding a global optimum via a branch-and-bound solver. In addition, using the MISDP reformulation, we extend the existing links between the considered $\ell_{2,0}$ -norm constrained problem and its commonly used convex relaxation — the $\ell_{2,1}$ -norm minimization problem. Lastly, we remark that, although, in this paper, the measurement model is described in an application of DOA estimation, the proposed method is not restricted to any specific dictionary structure and, therefore, can be directly applied to a joint sparse estimation problem in any other application.

To summarize, the main contributions of this paper are:

- *Problem reformulation:* We consider the MAP estimation of an MMV problem, which is formulated as a regularized LS problem with an $\ell_{2,0}$ -norm constraint, and derive an equivalent MISDP reformulation. The presented MISDP reformulation can be viewed as an extension of the reformulation in [39] to the MMV case. However, we provide a different interpretation of the reformulation.
- *Efficient solution approach:* In contrast to the DML estimator, which is obtained by brute-force search, the MAP estimator, as the global optimum of the MISDP reformulation, can be achieved by an efficient MISDP solver using a semidefinite programming (SDP) based branch-and-bound method at a significantly reduced computation time. Our approach has the attractive feature that, if the branch-and-bound solver is terminated early, an optimality assessment of the obtained solution is provided by the gap between the lower and upper bounds of the optimal value.
- *Large problem handling:* For problems of extremely

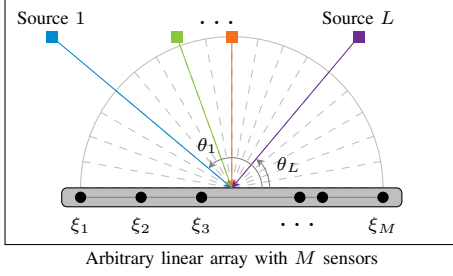


Fig. 1. Exemplary setup for a linear array of M sensors and L source signals.

large dimensions, we provide a randomized rounding algorithm, as an extension of the procedure proposed by Pilanci et al. in [39] for the SMV case, that can find a satisfactory approximate solution of the proposed MISDP reformulation at a practically affordable computation time.

- *Theoretical results:* Based on the MISDP reformulation, we extend the existing results on the theoretical links between the considered $\ell_{2,0}$ -norm constrained formulation and the commonly used convex formulation with the $\ell_{2,1}$ -norm regularization.

The paper is organized as follows. The sensor array signal model is presented in Section II. In Section III, we briefly review the DML estimator and the MAP estimator established in the Bayesian framework, as two classical multi-source estimation methods. In Section IV, the DOA estimation task is modeled as an MMV problem, and the equivalent MISDP reformulation is established. Two solution approaches for the MISDP reformulation are then described in Section V. In Section VI, using the developed reformulation, we provide a theoretical comparison between the $\ell_{2,0}$ -norm constrained problem and the conventional convex method with $\ell_{2,1}$ -norm minimization. In Section VII, we briefly introduce a generalization of the proposed MISDP-based method for the DOA estimation with nonuniform source variances. Simulation results are presented in Section VIII, and conclusions are drawn in Section IX.

Notation: We use x , \mathbf{x} , and \mathbf{X} to denote a scalar, column vector, and matrix, respectively. For any $x \in \mathbb{C}$, x^* denotes its complex conjugate. The sets of $M \times M$ Hermitian and positive semidefinite (PSD) Hermitian matrices are denoted by \mathbb{S}^M and \mathbb{S}_+^M , respectively. The $M \times M$ identity matrix is denoted by \mathbf{I}_M , and $\mathbf{0}$ and $\mathbf{1}$ represent a zero matrix and all-ones matrix, respectively. The symbols $(\cdot)^T$, $(\cdot)^H$, and $(\cdot)^{-1}$ denote the transpose, Hermitian transpose, and inverse, respectively. The trace operator is written as $\text{tr}(\cdot)$. The Frobenius norm and the $\ell_{p,q}$ -mixed-norm of a matrix \mathbf{X} , defined in (15), are referred to as $\|\mathbf{X}\|_F$ and $\|\mathbf{X}\|_{p,q}$, respectively, while the ℓ_p -norm of a vector is defined as $\|\mathbf{x}\|_p$. In particular, the ℓ_0 -pseudo-norm $\|\mathbf{x}\|_0$ counts the number of nonzero entries in the vector \mathbf{x} .

II. SIGNAL MODEL

As depicted in Fig. 1, we consider a linear array of M omnidirectional sensors. Assume that L narrowband far-field

source signals impinge from distinct directions $\theta_1, \dots, \theta_L \in [0, 180^\circ]$. The corresponding spatial frequencies are defined as

$$\mu_l = \pi \cos(\theta_l) \in [-\pi, \pi) \quad (1)$$

for $l = 1, \dots, L$ and summarized in the vector $\boldsymbol{\mu} = [\mu_1, \dots, \mu_L]^T$. We consider the DOA estimation problem with multiple snapshots, where the array output provides measurements recorded at N time instants. We assume that the sources emit time-varying signals, whereas the spatial frequencies in $\boldsymbol{\mu}$ remain constant within the entire observation time. Let $\mathbf{Y} = [\mathbf{y}_1, \dots, \mathbf{y}_N] \in \mathbb{C}^{M \times N}$ be the matrix that contains the N snapshots and, specifically, the (m, n) th entry $y_{m,n}$ is the output of sensor m at time instant n . The measurement matrix is modeled as

$$\mathbf{Y} = \mathbf{A}(\boldsymbol{\mu})\boldsymbol{\Psi} + \mathbf{N}, \quad (2)$$

where $\boldsymbol{\Psi} = [\boldsymbol{\psi}_1, \dots, \boldsymbol{\psi}_N] \in \mathbb{C}^{L \times N}$ is the source waveform matrix with $\boldsymbol{\psi}_{l,n}$ being the signal emitted by source l at time instant n . The matrix $\mathbf{A}(\boldsymbol{\mu})$ collects the L steering vectors as

$$\mathbf{A}(\boldsymbol{\mu}) = [\mathbf{a}(\mu_1) \quad \dots \quad \mathbf{a}(\mu_L)] \in \mathbb{C}^{M \times L}, \quad (3)$$

where $\mathbf{a}(\mu) = [e^{j\mu\xi_1}, \dots, e^{j\mu\xi_M}]^T$ is the steering vector corresponding to the frequency μ and ξ_1, \dots, ξ_M denote the sensor locations in the linear array measured in half-wavelength. Furthermore, the matrix $\mathbf{N} = [\mathbf{n}_1, \dots, \mathbf{n}_N] \in \mathbb{C}^{M \times N}$ represents independent and identically distributed (i.i.d.) circular and spatio-temporal white Gaussian noise with σ^2 being the variance of each noise entry $n_{m,n}$.

III. DETERMINISTIC MAXIMUM LIKELIHOOD AND MAXIMUM A POSTERIORI ESTIMATORS

In this section we briefly review the DML estimator and the MAP estimator established in the Bayesian framework, as two classical multi-source estimation methods. As those methods are often computationally demanding, e.g., if the number of sources is large, we propose an equivalent reformulation of the MAP estimation problem in Section IV. The resulting MISDP reformulation enables a computationally efficient solution to the MAP estimation problem using state-of-the-art numerical MISDP solvers.

In the deterministic maximum likelihood (DML) approach, the source waveform matrix $\boldsymbol{\Psi}$ in (2) is considered to be deterministic and unknown. According to the signal model in (2), the snapshots \mathbf{y}_n are statistically independent and complex normally distributed with mean $\mathbf{A}(\boldsymbol{\mu})\boldsymbol{\psi}_n$ and covariance matrix $\sigma^2 \mathbf{I}_M$, i.e.,

$$\mathbf{y}_n | \boldsymbol{\psi}_n \sim \mathcal{CN}(\mathbf{A}(\boldsymbol{\mu})\boldsymbol{\psi}_n, \sigma^2 \mathbf{I}_M). \quad (4)$$

Thus, the DML estimator for the frequencies $\boldsymbol{\mu}$ and the source waveforms $\boldsymbol{\Psi}$ is obtained as the solution of the following nonlinear LS problem [27]:

$$\min_{\boldsymbol{\mu} \in [-\pi, \pi)^L, \boldsymbol{\Psi} \in \mathbb{C}^{L \times N}} \|\mathbf{A}(\boldsymbol{\mu})\boldsymbol{\Psi} - \mathbf{Y}\|_F^2. \quad (5)$$

Since we are mainly interested in estimating the DOA parameters $\boldsymbol{\mu}$, the objective function in (5) can be concentrated with respect to the nuisance parameters $\boldsymbol{\Psi}$. That is, for each value of $\boldsymbol{\mu}$, the minimizer of the nuisance parameters $\boldsymbol{\Psi}$ can be

expressed in closed form, which can then be substituted into the original objective function to obtain the concentrated optimization problem. Particularly, the DML estimation problem in (5) can be concentrated as

$$\min_{\boldsymbol{\mu} \in [-\pi, \pi]^L} \text{tr} \left(\mathbf{Y}^H \boldsymbol{\Pi}_{\mathbf{A}(\boldsymbol{\mu})}^\perp \mathbf{Y} \right), \quad (6)$$

where $\boldsymbol{\Pi}_{\mathbf{A}(\boldsymbol{\mu})}^\perp = \mathbf{I}_M - \mathbf{A}(\boldsymbol{\mu}) (\mathbf{A}(\boldsymbol{\mu})^H \mathbf{A}(\boldsymbol{\mu}))^{-1} \mathbf{A}(\boldsymbol{\mu})^H$ denotes the orthogonal projector onto the orthogonal complement of the column space of the matrix $\mathbf{A}(\boldsymbol{\mu})$.

The maximum a posteriori (MAP) estimator [20], [28] developed in the Bayesian framework is another widely used estimation method that is closely related to the ML estimation. In this approach, only the DOAs are considered to be deterministic, whereas the source waveforms are assumed to be stochastic. In particular, we consider the spatio-temporal i.i.d. assumption that the signal waveforms $\psi_{l,n}$ are statistically independent for different sources and snapshots. They follow the same circularly-symmetric complex Gaussian distribution

$$\psi_n \sim \mathcal{CN}(\mathbf{0}, \gamma \mathbf{I}_L), \quad (7)$$

where γ is the source power that is assumed to be known a priori. By the Bayes' rule, the MAP estimator for the uncorrelated Gaussian prior in (7) is given by the solution of the following regularized LS problem [20]:

$$\begin{aligned} & \max_{\boldsymbol{\mu} \in [-\pi, \pi]^L, \boldsymbol{\Psi} \in \mathbb{C}^{L \times N}} \prod_{n=1}^N p(\psi_n | \mathbf{y}_n) \\ \Leftrightarrow & \max_{\boldsymbol{\mu} \in [-\pi, \pi]^L, \boldsymbol{\Psi} \in \mathbb{C}^{L \times N}} \prod_{n=1}^N p(\mathbf{y}_n | \psi_n) p(\psi_n) \end{aligned} \quad (8a)$$

$$\begin{aligned} \Leftrightarrow & \min_{\boldsymbol{\mu} \in [-\pi, \pi]^L, \boldsymbol{\Psi} \in \mathbb{C}^{L \times N}} \sum_{n=1}^N -\log(p(\mathbf{y}_n | \psi_n)) - \log(p(\psi_n)) \\ \Leftrightarrow & \min_{\boldsymbol{\mu} \in [-\pi, \pi]^L, \boldsymbol{\Psi} \in \mathbb{C}^{L \times N}} \|\mathbf{A}(\boldsymbol{\mu}) \boldsymbol{\Psi} - \mathbf{Y}\|_F^2 + \rho \|\boldsymbol{\Psi}\|_F^2, \end{aligned} \quad (8b)$$

where $p(\cdot)$ denotes the probability density function and

$$\rho = \sigma^2 / \gamma. \quad (9)$$

The first LS data fitting term in (8b) resulting from the likelihood $p(\mathbf{y}_n | \psi_n)$ is identical to the DML cost function in (5), whereas the prior distribution $p(\psi_n)$, according to the Gaussian assumption in (7), introduces the Tikhonov regularization term in (8b). For a given vector $\boldsymbol{\mu}$, the minimizer of the nuisance parameters $\boldsymbol{\Psi}$ in problem (8) admits the well-known Tikhonov closed-form solution [43]

$$\tilde{\boldsymbol{\Psi}} = (\mathbf{A}(\boldsymbol{\mu})^H \mathbf{A}(\boldsymbol{\mu}) + \rho \mathbf{I}_L)^{-1} \mathbf{A}(\boldsymbol{\mu})^H \mathbf{Y}. \quad (10)$$

Then, by substituting (10) into (8), the MAP estimation can be concentrated as

$$\min_{\boldsymbol{\mu} \in [-\pi, \pi]^L} \text{tr} \left(\mathbf{Y}^H \tilde{\boldsymbol{\Pi}}_{\mathbf{A}(\boldsymbol{\mu})}^\perp \mathbf{Y} \right) \quad (11)$$

with $\tilde{\boldsymbol{\Pi}}_{\mathbf{A}(\boldsymbol{\mu})}^\perp = \mathbf{I}_M - \mathbf{A}(\boldsymbol{\mu}) (\mathbf{A}(\boldsymbol{\mu})^H \mathbf{A}(\boldsymbol{\mu}) + \rho \mathbf{I}_L)^{-1} \mathbf{A}(\boldsymbol{\mu})^H$. Moreover, by using the matrix inversion lemma, the matrix $\tilde{\boldsymbol{\Pi}}_{\mathbf{A}(\boldsymbol{\mu})}^\perp$ can be rewritten as $\tilde{\boldsymbol{\Pi}}_{\mathbf{A}(\boldsymbol{\mu})}^\perp = (\frac{1}{\rho} \mathbf{A}(\boldsymbol{\mu}) \mathbf{A}(\boldsymbol{\mu})^H + \mathbf{I}_M)^{-1}$, which leads to the following equivalent expression of the concentrated MAP estimation in (11):

$$\min_{\boldsymbol{\mu} \in [-\pi, \pi]^L} \text{tr} \left(\mathbf{Y}^H \left(\frac{1}{\rho} \mathbf{A}(\boldsymbol{\mu}) \mathbf{A}(\boldsymbol{\mu})^H + \mathbf{I}_M \right)^{-1} \mathbf{Y} \right). \quad (12)$$

IV. A MISDP REFORMULATION OF MAP ESTIMATION FOR THE MMV PROBLEM

Due to the quadratic term in the matrix inversion, both the DML and the MAP estimation problems in (6) and (12), respectively, are nonconvex and multimodal with a large number of local minima. Hence, the corresponding optimization procedure is computationally demanding and generally requires a multidimensional grid search to find the exact solution. Inspired by the concept of compressed sensing [35], the above DOA estimation problem can be modeled as an MMV problem by introducing a predefined dictionary that samples the complete FOV [36]. In this section, we first introduce the MMV-based model for DOA estimation. Then, for the MMV problem, a dictionary-based MAP estimation problem is developed according to (8), which can be reformulated as a MISDP problem by the reformulation techniques in [14], [39].

The problem of recovering the frequencies in $\boldsymbol{\mu}$ from the measurement matrix \mathbf{Y} can be formulated as an MMV problem by exploiting the following sparse representation for the model in (2):

$$\mathbf{Y} = \mathbf{A}(\boldsymbol{\nu}) \mathbf{X} + \mathbf{N}, \quad (13)$$

where $\mathbf{A}(\boldsymbol{\nu}) = [\mathbf{a}(\nu_1), \dots, \mathbf{a}(\nu_K)] \in \mathbb{C}^{M \times K}$ is an overcomplete dictionary constructed by sampling the FOV in $K \gg L$ directions with spatial frequencies $\boldsymbol{\nu} = [\nu_1, \dots, \nu_K]^T$ and $\mathbf{X} \in \mathbb{C}^{K \times N}$ is a sparse representation of the source signal matrix $\boldsymbol{\Psi}$. Specifically, provided that the true frequencies $\boldsymbol{\mu}$ are contained in the frequency grid, i.e.,

$$\{\mu_l\}_{l=1}^L \subset \{\nu_k\}_{k=1}^K, \quad (14)$$

then $\mathbf{X} = [\mathbf{x}_1, \dots, \mathbf{x}_K]^T$ admits a row-sparse structure, which has only L nonzero rows corresponding to the signal waveforms of the L sources, i.e., $\mathbf{A}(\boldsymbol{\mu}) \boldsymbol{\Psi} = \mathbf{A}(\boldsymbol{\nu}) \mathbf{X}$. Thus, the considered DOA estimation problem can be described as an MMV problem, which aims at jointly recovering a set of signal samples in \mathbf{X} that have common sparse support over a given dictionary $\mathbf{A}(\boldsymbol{\nu})$ from multiple measurement vectors in \mathbf{Y} . The spatial frequencies are then estimated from the support of the recovered row-sparse signal matrix $\hat{\mathbf{X}} = [\hat{\mathbf{x}}_1, \dots, \hat{\mathbf{x}}_K]^T$ by $\{\hat{\mu}_l\}_{l=1}^L = \{\nu_k \mid \|\hat{\mathbf{x}}_k\|_0 > 0, k = 1, \dots, K\}$. For simplicity, in the rest of the paper, the dictionary is referred to as $\mathbf{A} = \mathbf{A}(\boldsymbol{\nu})$.

The $\ell_{p,q}$ -mixed-norms are commonly used to enforce the row-sparsity assumption in sparse reconstruction problems [15]. Specifically, the $\ell_{p,q}$ -norm for a matrix $\mathbf{X} = [\mathbf{x}_1, \dots, \mathbf{x}_K]^T$ is defined as

$$\|\mathbf{X}\|_{p,q} = \|\mathbf{x}^{(\ell_p)}\|_q \quad \text{with} \quad \mathbf{x}^{(\ell_p)} = [\|\mathbf{x}_1\|_p \cdots \|\mathbf{x}_K\|_p]^T. \quad (15)$$

The inner ℓ_p -norm applied to each row provides a nonlinear coupling among the elements in a row, whereas the outer ℓ_q -norm applied to the norms of all rows approximately measures the row-sparsity. In particular, the $\ell_{p,0}$ -pseudo-norm represents the exact number of nonzero rows of the matrix, which, however, typically leads to an NP-hard problem due to its nonconvexity. In [13], the $\ell_{2,1}$ -norm is utilized as a convex approximation of the $\ell_{2,0}$ -norm, to address the MMV problem

described above. In contrast, in this paper, we consider the exact MAP estimation for the sparse model in (13).

Let us impose the same spatio-temporal i.i.d. zero-mean complex Gaussian prior assumption in (7) on the nonzero rows of the matrix \mathbf{X} . Therefore, the entries $x_{k,n}$ in the nonzero rows of \mathbf{X} are independent both across snapshots and across DOAs and follow the distribution

$$x_{k,n} \sim \mathcal{CN}(0, \gamma) \quad (16)$$

for $n = 1, \dots, N$. Then, similar to (8), the MAP estimator for the sparse model in (13) is given by the following regularized LS problem with $\ell_{2,0}$ -norm constraint:

$$\min_{\mathbf{X} \in \mathbb{C}^{K \times N}, \|\mathbf{X}\|_{2,0} \leq L} \|\mathbf{A}\mathbf{X} - \mathbf{Y}\|_F^2 + \rho \|\mathbf{X}\|_F^2. \quad (17)$$

The DML approach for the sparse model in (13) is obtained from (17) by choosing the regularization parameter ρ to be zero. The problem (17) is equivalent to solving the MAP estimation problem (8b) via a brute-force search over the spatial frequency grid in (14). Note that, to be consistent with (8b), \mathbf{X} is not restricted to have exactly L nonzero rows, i.e., $\|\mathbf{X}\|_{2,0} = L$, since the waveforms in (8b) can also attain zero values for any chosen combination of spatial frequencies $\boldsymbol{\mu}$. However, compared to the DML approach, the MAP estimation in (17) can be equivalently reformulated as a MISDP problem due to the additional Tikhonov regularization, and then, its global optimum can be conveniently obtained by a state-of-the-art MISDP solver. Problem (17) with the $\ell_{2,0}$ -norm constraint can be viewed as a generalization of the ℓ_0 -norm constrained LS regression problem for a single measurement, as considered by Pilanci et al. in [39], to the MMV case. In this paper, we provide a nontrivial extension of Pilanci's MISDP reformulation for the SMV case to the MMV problem (17). The regularization parameter ρ is chosen according to (9) if the prior information of the expected power of the source waveforms is known and satisfies the assumption in (7). Otherwise, if training data are available, a suitable value of ρ may be obtained through cross-validation or, more efficiently, with the help of the algorithm unrolling procedure [44]. On the other hand, the parameter ρ also has a significant influence on the running time of the two solution approaches for problem (17) that will be introduced in Section V. As can be easily observed, a larger value of ρ leads to a better-conditioned problem, which can generally be solved faster. Therefore, if no prior information is available, one may simply choose ρ to be as small as possible under a given running time limit, in order to achieve a good approximation of the DML estimator with the efficient solution approaches presented in Section V.

In the following, we present a simplified derivation of the MISDP reformulation for the MMV case, which, unlike that in [39], does not involve the dual problem constructed with the Legendre-Fenchel conjugate. Instead, we justify the equivalence of the MISDP reformulation by the concentration with respect to the nuisance parameters in the primal domain. First, by introducing additional binary variables $\mathbf{u} \in \{0, 1\}^K$,

the original $\ell_{2,0}$ -norm constrained problem in (17) can be equivalently represented as the lifted problem

$$\min_{\substack{\mathbf{u} \in \{0,1\}^K \\ \mathbf{u}^\top \mathbf{1} \leq L}} \min_{\mathbf{X} \in \mathbb{C}^{K \times N}} \|\mathbf{A}\mathbf{D}(\mathbf{u})\mathbf{X} - \mathbf{Y}\|_F^2 + \rho \|\mathbf{X}\|_F^2. \quad (18)$$

The matrix $\mathbf{D}(\mathbf{u})$ in (18) is a diagonal matrix with \mathbf{u} on its main diagonal, which determines the active directions in the dictionary \mathbf{A} , i.e., the directions with nonzero source signals. Note that $\mathbf{D}(\mathbf{u})$ is not required in the regularization in (18) because the rows of \mathbf{X} that are not selected by $\mathbf{D}(\mathbf{u})$ are not involved in the data fitting term and, hence, will be enforced to be all-zero by the minimization of $\|\mathbf{X}\|_F^2$. Like the MAP estimation in (8), problem (18) can also be concentrated with respect to \mathbf{X} and then reformulated by the matrix inversion lemma as the following integer program (IP)

$$\min_{\mathbf{u} \in \{0,1\}^K, \mathbf{u}^\top \mathbf{1} \leq L} \text{tr} \left(\mathbf{Y}^H \left(\frac{1}{\rho} \mathbf{A}\mathbf{D}(\mathbf{u})\mathbf{A}^H + \mathbf{I}_M \right)^{-1} \mathbf{Y} \right). \quad (19)$$

Next, by applying the same SDP reformulation technique as in [14], [39], the integer program in (19) can be further written as the following MISDP problem with a slack variable \mathbf{T} :

$$\min_{\mathbf{u} \in \{0,1\}^K, \mathbf{T} \in \mathbb{S}_+^M} \text{tr}(\mathbf{T}) \quad (20a)$$

$$\text{s.t.} \quad \begin{bmatrix} \frac{1}{\rho} \mathbf{A}\mathbf{D}(\mathbf{u})\mathbf{A}^H + \mathbf{I}_M & \mathbf{Y} \\ \mathbf{Y}^H & \mathbf{T} \end{bmatrix} \succeq 0, \quad (20b)$$

$$\mathbf{u}^\top \mathbf{1} \leq L. \quad (20c)$$

Note that the positive semidefiniteness of the matrix \mathbf{T} is enforced by the PSD constraint (20b). The equivalence of the two problems in (19) and (20) can be shown as follows. Since $\frac{1}{\rho} \mathbf{A}\mathbf{D}(\mathbf{u})\mathbf{A}^H + \mathbf{I}_M$ is positive definite, by the Schur complement formula, the constraint (20b) is equivalent to [45]

$$\mathbf{T} \succeq \mathbf{Y}^H \left(\frac{1}{\rho} \mathbf{A}\mathbf{D}(\mathbf{u})\mathbf{A}^H + \mathbf{I}_M \right)^{-1} \mathbf{Y}.$$

Therefore, for every given \mathbf{u} , the minimum of $\text{tr}(\mathbf{T})$ in (20) is achieved at $\mathbf{T} = \mathbf{Y}^H \left(\frac{1}{\rho} \mathbf{A}\mathbf{D}(\mathbf{u})\mathbf{A}^H + \mathbf{I}_M \right)^{-1} \mathbf{Y}$. The above argument also exhibits the fact that the solution of the MISDP problem (20) is completely determined as long as the optimal solution of the binary variable \mathbf{u} is given.

It can be observed that the dimension of the semidefinite constraint (20b) is proportional to the number of snapshots N , which becomes computationally demanding for the case with a large number of snapshots. Therefore, following a similar line of analysis as in SPARROW [14], we derive another equivalent MISDP formulation that scales better with respect to N . The objective function in problem (19) depends only on the sample covariance matrix of the received signals $\hat{\mathbf{R}} = \frac{1}{N} \mathbf{Y}\mathbf{Y}^H$ and, hence, can be rewritten as follows:

$$\begin{aligned} & \text{tr} \left(\mathbf{Y}^H \left(\frac{1}{\rho} \mathbf{A}\mathbf{D}(\mathbf{u})\mathbf{A}^H + \mathbf{I}_M \right)^{-1} \mathbf{Y} \right) \\ &= N \text{tr} \left(\left(\frac{1}{\rho} \mathbf{A}\mathbf{D}(\mathbf{u})\mathbf{A}^H + \mathbf{I}_M \right)^{-1} \hat{\mathbf{R}} \right) \\ &= \text{tr} \left(\hat{\mathbf{Y}}^H \left(\frac{1}{\rho} \mathbf{A}\mathbf{D}(\mathbf{u})\mathbf{A}^H + \mathbf{I}_M \right)^{-1} \hat{\mathbf{Y}} \right), \end{aligned} \quad (21)$$

where $\hat{\mathbf{Y}} = \sqrt{N} \cdot \hat{\mathbf{R}}^{\frac{1}{2}} \in \mathbb{C}^{M \times M}$. It then leads to the following equivalent MISDP formulation:

$$\min_{\mathbf{u} \in \{0,1\}^K, \mathbf{T} \in \mathbb{S}_+^M} \text{tr}(\mathbf{T}) \quad (22a)$$

$$\text{s.t.} \quad \begin{bmatrix} \frac{1}{\rho} \mathbf{A} \mathbf{D}(\mathbf{u}) \mathbf{A}^H + \mathbf{I}_M & \hat{\mathbf{Y}} \\ \hat{\mathbf{Y}}^H & \mathbf{T} \end{bmatrix} \succeq 0, \quad (22b)$$

$$\mathbf{u}^T \mathbf{1} \leq L. \quad (22c)$$

In contrast to the constraint (20b), the dimension of the semidefinite constraint (22b) is independent of the number of snapshots N . In summary, either formulation (20) or (22) can be used to solve the $\ell_{2,0}$ -norm constrained problem in (17), depending on the number of snapshots N . Specifically, (20) is preferable in the undersampled case, i.e., $N \leq M$, and (22) is preferable otherwise.

V. SOLUTION APPROACHES FOR THE MISDP REFORMULATION

The MISDP implementation (20) or (22) of the considered MMV problem can be directly solved by a general purpose MISDP solver such as SCIP-SDP [40]–[42]. The SCIP-SDP solver provides two efficient approaches based on the widely used branch-and-bound method and cutting-plane method, respectively. Both the branch-and-bound and the cutting-plane approaches admit an improved scalability in the case of a large problem dimension, compared to the simple brute-force search on the integer variables. Compared to this setting, the branch-and-bound method, even if terminated early, provides an optimality assessment of the obtained solution by the gap between the lower and upper bounds of the optimal value. The branch-and-bound and the cutting-plane approaches require iteratively either solving continuous SDP relaxations or the computation of an eigendecomposition for the construction of cutting planes [40]. Hence, the SCIP-SDP solver may also become computationally demanding with the increase of the problem dimension due to the increase of both the number of required nodes in the branch-and-bound tree and cutting planes and the computational complexity of each subproblem.

In contrast to solving the MISDP reformulation exactly, in [39], the authors present a low-complexity method for obtaining a good approximate solution in the case with a single measurement vector, which is based on the randomized rounding (RR) technique. The method can be generalized to the MMV case and it consists of two main steps, namely, the interval relaxation and the randomized rounding, which is outlined in Algorithm 1. The interval relaxation in Step 1 is a continuous SDP and can be efficiently solved by a generic interior-point solver such as MOSEK [46]. To further reduce the complexity of Step 1 in the case of an extremely large problem dimension, one may consider an attractive alternative that, instead of solving the interval relaxation of the MISDP formulation in (20) with interior-point solvers, employs projected first-order and quasi-Newton methods [47], or primal-dual methods such as ADMM [48] to solve the interval relaxation of the equivalent IP formulation in (19). When the optimal solution $\hat{\mathbf{u}}$ of the interval relaxation is binary, then it is also the optimal solution of the original

Algorithm 1: The Randomized Rounding (RR) Algorithm for the MISDP Problem (20) or (22).

- Step 1** *Interval Relaxation:* Solve the convex relaxation of the MISDP formulation in (20) or (22) that replaces the Boolean hypercube $\{0,1\}^K$ by its convex hull, the unit hypercube $[0,1]^K$. Let $\hat{\mathbf{u}} \in [0,1]^K$ be the optimal solution of the relaxed problem.
- Step 2** *Randomized Rounding:* Given the approximate solution $\hat{\mathbf{u}}$, randomly generate $T > 0$ binary solutions $\tilde{\mathbf{u}} \in \{0,1\}^K$ where each entry \tilde{u}_k independently follows the Bernoulli distribution $\mathbb{P}[\tilde{u}_k = 1] = \hat{u}_k$ and $\mathbb{P}[\tilde{u}_k = 0] = 1 - \hat{u}_k$ for $k = 1, \dots, K$. An infeasible binary solution with $\tilde{\mathbf{u}}^T \mathbf{1} > L$ is afterward projected to the feasible set by retaining only the L ones in $\tilde{\mathbf{u}}$ with the largest values in the fractional solution $\hat{\mathbf{u}}$. Then, the solution $\tilde{\mathbf{u}}^*$ with the smallest objective function value, which can be calculated according to the IP formulation in (19), among all feasible solutions is chosen to be the approximate solution.
-

MISDP problem. Additional analyses of the conditions for the interval relaxation to have a binary solution are provided in [39] in the SMV case with random dictionaries.

Otherwise, if the solution $\hat{\mathbf{u}}$ is not binary, the randomized rounding technique is employed to efficiently search for a good binary solution. The basic randomized rounding procedure, which is used in [39], searches in a set of $T > 0$ randomly generated independent and identically distributed (i.i.d.) binary solutions $\tilde{\mathbf{u}} \in \{0,1\}^K$ where each entry \tilde{u}_k independently follows the Bernoulli distribution with the success probability

$$\mathbb{P}[\tilde{u}_k = 1] = \hat{u}_k. \quad (23)$$

The motivation for using the fractional solution as the probability of the corresponding binary variable taking the value one is as follows. First, the fractional solution is restricted to be in the interval $[0,1]$. Second, the solution of the continuous relaxation is expected to be close to the solution of the original integer program, which relies on the tightness of the relaxation. In particular, several bounds on the disparity between the optimal value of the interval relaxation and that of the original problem have been established for the class of binary integer linear programs [49]–[51]. Although a theoretical guarantee on the tightness of the interval relaxation for the considered MISDP problem has not been derived, the numerical simulations in Section VIII demonstrate that the randomized rounding procedure is capable of finding good approximate solutions for the considered MISDP problem with reasonable choices of T .

The cardinality of a binary solution $\tilde{\mathbf{u}}$ generated according to the distribution (23) follows a Poisson binomial distribution with the expectation $\mathbb{E}[\tilde{\mathbf{u}}^T \mathbf{1}] = \hat{\mathbf{u}}^T \mathbf{1} \leq L$. If the expected sparsity level L is consistent with the ground truth, the interval relaxation, as well as the original integer program, is expected

to attain the optimum at the boundary of the constraint set $\{\mathbf{u} \mid \mathbf{u}^\top \mathbf{1} \leq L\}$. In this case, i.e., when $\hat{\mathbf{u}}^\top \mathbf{1} = L$, a drawback of the basic randomized rounding procedure is that the probability of generating an infeasible binary solution, i.e., $\mathbb{P}[\hat{\mathbf{u}}^\top \mathbf{1} > L]$, is still high. Of course, one may simply increase the total number T of binary solutions to be generated to explore a sufficient number of feasible binary solutions. Alternatively, an extended version of the randomized rounding with the scaling technique is proposed in [49] for reducing the failure probability $\mathbb{P}[\hat{\mathbf{u}}^\top \mathbf{1} > L]$. In short, it uses a down-scaled version $(1 - \delta)\hat{\mathbf{u}}$, with $\delta \in (0, 1)$, of the fractional solution, rather than directly $\hat{\mathbf{u}}$, as the probabilities for the generation of binary solutions. It follows that the expected cardinality of the generated binary solutions does not exceed $(1 - \delta)L$. A required upper bound on the failure probability $\mathbb{P}[\hat{\mathbf{u}}^\top \mathbf{1} > L]$ can be satisfied by properly choosing the scaling parameter δ . Nevertheless, since random samples typically concentrate on the expectation, more binary solutions in the interior of the constraint set $\{\mathbf{u} \mid \mathbf{u}^\top \mathbf{1} \leq L\}$ are explored by down-scaling the probabilities. As we consider the case where the expected sparsity level L is consistent with the ground truth, it is instead beneficial to test more binary solutions at the boundary of the constraint set, i.e., with a cardinality of exactly L . To this end, we propose a different extended version of randomized rounding with a subsequent projection step. Specifically, as described in Algorithm 1, instead of discarding the generated infeasible binary solutions, i.e., the binary solutions with cardinality larger than L , we further project each infeasible binary solution to the constraint set by preserving only L ones with the largest probabilities, i.e., the values in the fractional solution $\hat{\mathbf{u}}$. Consistent with the above analysis, the proposed RR with projection often finds a binary solution that provides a lower objective function value even with fewer randomly explored binary solutions compared to the basic RR and RR with scaling.

The IP formulation (19) established on the sparse signal model (13) is equivalent to solving the concentrated MAP estimation problem (12) via a brute-force search over the frequency grid $\{\nu_k\}_{k=1}^K$. Compared to the objective function in (12), the equivalent expression in (11) admits a lower computational complexity since the number of sources L is generally much smaller than the array size M . Therefore, the evaluation of the objective function in (19) at a randomly generated binary solution $\tilde{\mathbf{u}}$ in the randomized rounding can be more efficiently performed according to the objective function in (11), where the steering matrix $\mathbf{A}(\boldsymbol{\mu})$ is determined by the columns in the dictionary $\mathbf{A}(\boldsymbol{\nu})$ selected by $\tilde{\mathbf{u}}$.

We remark that a basic randomized rounding procedure without the subsequent projection step in Algorithm 1 is employed internally by SCIP-SDP to find good integer solutions for the estimation of the upper bounds of the optimal value in the branch-and-bound approach. Similar to other branch-and-bound methods, SCIP-SDP typically finds an optimal or near-optimal solution rapidly. However, it requires significantly more time to verify the optimality of this solution through lower bound computations. This observation also motivates the idea of using the randomized rounding Algorithm 1 for obtaining a good approximate solution of the considered

MISDP problem at a low computational cost.

Furthermore, the on-grid assumption (14) is typically not fulfilled in practice due to the finite grid size, which results in spectral leakage effects and basis mismatch [52], [53] in the reconstructed signal. To depress the grid mismatch error, one may perform an additional local search step that employs a generic, e.g., based on gradient methods, or customized, e.g., the alternating projection algorithm in [54], local optimization solver to find a local optimum of the gridless DML estimation in (6) or the gridless MAP estimation in (11), starting from the frequencies recovered by the grid-based method. Nevertheless, since it finds only a local optimum, it is not guaranteed to always improve the estimation quality, especially if the frequencies recovered by the grid-based method are very poor.

VI. RELATION TO THE $\ell_{2,1}$ -NORM MINIMIZATION

In the literature, the ℓ_1 -norm is widely used as a convex approximation of the ℓ_0 -norm for obtaining computationally more tractable problems [18], [19]. In the MMV case, the following $\ell_{2,1}$ -norm minimization problem [13]

$$\min_{\mathbf{X} \in \mathbb{C}^{N \times K}} \frac{1}{2} \|\mathbf{A}\mathbf{X} - \mathbf{Y}\|_F^2 + \lambda \sqrt{N} \|\mathbf{X}\|_{2,1} \quad (24)$$

is typically considered as a generalization of the classic ℓ_1 -norm minimization problem, where $\lambda > 0$ is a regularization parameter. To address problem (24), the SPARROW method in [14] utilizes the following equivalent convex reformulation:

$$\min_{\mathbf{s} \in \mathbb{R}_+^K} \text{tr} \left((\mathbf{A}\mathbf{D}(\mathbf{s})\mathbf{A}^H + \lambda \mathbf{I}_M)^{-1} \hat{\mathbf{R}} \right) + \mathbf{s}^\top \mathbf{1}. \quad (25)$$

The optimal solutions $\hat{\mathbf{X}} = [\hat{\mathbf{x}}_1, \dots, \hat{\mathbf{x}}_K]^\top$ and $\hat{\mathbf{s}}$ for (24) and (25), respectively, are related by $\hat{s}_k = \frac{1}{\sqrt{N}} \|\hat{\mathbf{x}}_k\|_2$ for $k = 1, \dots, K$. Similarly, problem (25) can be further reformulated as an SDP problem and solved by a generic SDP solver. Alternatively, a coordinate descent algorithm is also devised in [14] for problem (25), which is more scalable in the case with a large number of sensors M . By the expression in (21), the integer program (19) employed in our proposed method can be rewritten as

$$\min_{\mathbf{u} \in \{0,1\}^K, \mathbf{u}^\top \mathbf{1} \leq L} \text{tr} \left((\mathbf{A}\mathbf{D}(\mathbf{u})\mathbf{A}^H + \rho \mathbf{I}_M)^{-1} \hat{\mathbf{R}} \right), \quad (26)$$

where some constant factors are discarded. Thus, it can be concluded that problem (25) is equivalent to a Lagrangian of a convex continuous relaxation of the integer program in (26) where, in contrast to the interval relaxation used by the randomized rounding Algorithm 1, the binary variables are further relaxed to be nonnegative. As shown by the simulations in Section VIII, the continuous relaxation and Lagrangian relaxation lead to a degradation of the estimation quality, compared to our proposed method.

VII. GENERALIZATION TO THE SPARSE MAP ESTIMATION WITH NONUNIFORM SOURCE VARIANCES

In Section IV, we developed a MISDP reformulation for the sparse MAP estimation problem (17) with the uniform prior assumption in (16) where a priori the sources in all directions are assumed to have the same variance. In this section, we

consider the sparse MAP estimation problem with nonuniform source variances and briefly introduce a generalization of the MISDP-based method in Section IV.

Consider the sparse model in (13) constructed by sampling the FOV. The waveform matrix \mathbf{X} is similarly assumed to be row-sparse and follow a spatial-temporal i.i.d. zero-mean complex Gaussian distribution. However, unlike the uniform prior assumption in (16), the source variances are assumed to vary across the DOAs. Specifically, if there exists a source in the sampled direction with the spatial frequency ν_k , then the entries $x_{k,n}$ are assumed to follow the distribution

$$x_{k,n} \sim \mathcal{CN}(0, \gamma_k) \quad (27)$$

for $n = 1, \dots, N$, where $\gamma_k > 0$ denotes the given potential source variance in the DOA with the spatial frequency ν_k . The vector $\boldsymbol{\gamma} = [\gamma_1, \dots, \gamma_K]^T$ can be considered as the sampled spatial source power spectrum over the FOV, which may be estimated a priori by, e.g., the conventional beamforming or the SBL method. Define the regularization parameters

$$\rho_k = \sigma^2 / \gamma_k \quad (28)$$

for $k = 1, \dots, K$ and summarize them in the vector $\boldsymbol{\rho} = [\rho_1, \dots, \rho_K]^T$. Then, using the same considerations as in Section IV, we can write the sparse MAP estimation problem corresponding to the nonuniform prior in (27) as the following sparse LS problem with a row-wise weighted Tikhonov regularization

$$\min_{\substack{\mathbf{u} \in \{0,1\}^K \\ \mathbf{u}^T \mathbf{1} \leq L}} \min_{\mathbf{X} \in \mathbb{C}^{K \times N}} \|\mathbf{A}\mathbf{D}(\mathbf{u})\mathbf{X} - \mathbf{Y}\|_F^2 + \|\mathbf{D}(\sqrt{\boldsymbol{\rho}})\mathbf{X}\|_F^2, \quad (29)$$

where the square root operation is performed elementwise and ρ_k represents the regularization weight for the squared Euclidean norm of the k th row of \mathbf{X} . Similar to problem (18), the matrix $\mathbf{D}(\mathbf{u})$ is not required in the regularization in (29) because the rows of \mathbf{X} that are not selected by $\mathbf{D}(\mathbf{u})$ are not involved in the data fitting term and will be enforced to be all-zero by the minimization of the row norm.

Likewise, problem (29) can be concentrated with respect to \mathbf{X} and then reformulated by the matrix inversion lemma as the following integer program

$$\min_{\substack{\mathbf{u} \in \{0,1\}^K \\ \mathbf{u}^T \mathbf{1} \leq L}} \text{tr}(\mathbf{Y}^H(\mathbf{A}\mathbf{D}(\mathbf{u} \odot \boldsymbol{\rho})\mathbf{A}^H + \mathbf{I}_M)^{-1}\mathbf{Y}), \quad (30)$$

where \odot denotes the elementwise division. The integer program in (30) can be further written as MISDP problems similar to (20) and (22) by applying the same reformulation technique as in Section IV. Likewise, the MISDP reformulation is solved exactly by the SCIP-SDP solver or approximately by the randomized rounding Algorithm 1, as discussed in Section V. The details of the generalization of the MISDP reformulation and the solution approach for the sparse MAP estimation problem in (29) with nonuniform source variances are omitted due to space limitations.

VIII. SIMULATION RESULTS

In this section, we conduct numerical experiments on synthetic data to evaluate and analyze the performance of the proposed method, including both solution approaches introduced

in Section V for the MISDP reformulation. Specifically, the SCIP-SDP solver [40]–[42] of version 4.1.0 is used and the nonlinear branch-and-bound approach is chosen in the SCIP-SDP solver, where the relaxed continuous SDP subproblems are solved by MOSEK [46] of version 10.0.38.¹ The additional gridless local search described in Section V is achieved by the `fmincon` solver with the interior-point algorithm provided by MATLAB. The continuous SDP problem in the randomized rounding Algorithm 1 is modeled by using CVX [55], [56] and also solved by MOSEK. The estimation error of the proposed method is compared to the stochastic Cramér-Rao Bound (CRB) [57] and the estimation error of several widely used approaches for DOA estimation, namely, MUSIC [31], root-MUSIC [32], the SPARROW method with coordinate descent implementation, the sparse Bayesian learning (SBL) method in [17], and the DML estimator. The DML estimator is obtained via a brute-force search over the same grid as in (13), which is equivalent to the solution of problem (17) with the regularization parameter ρ being zero. The SBL method in [17] also employs an uncorrelated Gaussian prior assumption. However, in the SBL method, the source variances in the prior are not assumed to be known but, as mentioned in Section I, estimated by a type-II maximum likelihood method. The frequencies corresponding to the L largest peaks in the spectrum of the estimated source variances are then chosen to be the estimated frequencies. The results are averaged over $N_R = 1000$ Monte-Carlo trials unless otherwise noted. In particular, the quality of the estimated spatial frequencies $\hat{\boldsymbol{\mu}}(n) = [\hat{\mu}_1(n), \dots, \hat{\mu}_L(n)]^T$ for $n = 1, \dots, N_R$ are measured by the root-mean-square error (RMSE) with respect to the ground-truth $\boldsymbol{\mu}$ defined as

$$\text{RMSE}(\hat{\boldsymbol{\mu}}) = \sqrt{\frac{1}{LN_R} \sum_{n=1}^{N_R} \sum_{l=1}^L |\hat{\mu}_l(n) - \mu_l|_{\text{wa}}^2}, \quad (31)$$

where $|\mu_1 - \mu_2|_{\text{wa}} = \min_{k \in \mathbb{Z}} |\mu_1 - \mu_2 + 2k\pi|$ denotes the wrap-around distance between two frequencies μ_1 and μ_2 . All experiments were conducted on a Linux PC with an Intel Core i7-7700 CPU and 32 GB RAM running MATLAB 2024a.

In the simulations, we consider a ULA of $M = 8$ sensors with half-wavelength inter-element spacing, and the dictionary \mathbf{A} is constructed with $K = 100$ grid points with frequencies uniformly sampled in $[-\pi, \pi)$. The SNR is calculated as $\text{SNR} = 1/\sigma^2$.

Some algorithmic parameters are set as follows. The regularization parameter ρ in (17) for our proposed method is chosen according to the rule in (9) and the parameter λ in (24) for the SPARROW method is selected by the heuristic rule

$$\lambda = \sqrt{\sigma^2 M \log M} \quad (32)$$

as recommended in [14], [58]. The number T of randomly generated binary solutions in the randomized rounding algorithm is set to be 10^4 for $L = 3$ sources and 10^5 for $L = 5$ since the number of feasible binary solutions for problem (20) increases exponentially with increasing L . Also, when only

¹The source code of SCIP-SDP and an interface for MATLAB can be downloaded from the website <https://www.opt.tu-darmstadt.de/scipsdp>. In the experiments, the SCIP-SDP solver is called from MATLAB through the provided interface.

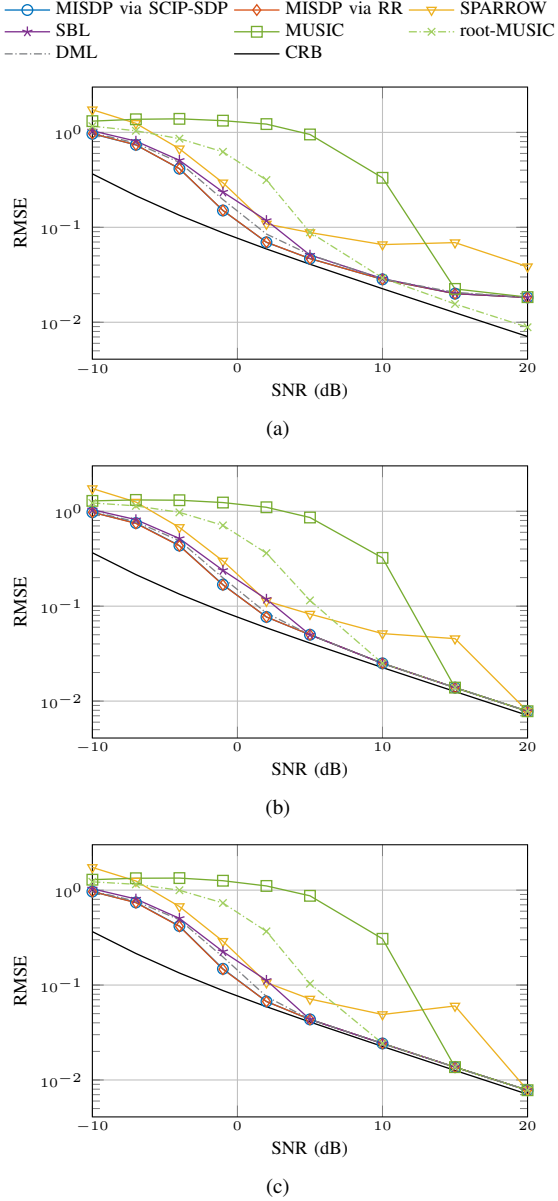


Fig. 2. Error performance w.r.t. SNR for $L = 3$ uncorrelated sources, $M = 8$ sensors, $N = 8$ snapshots, and $K = 100$ grid points, in the case (a) without gridless local search, (b) with gridless local search on the DML function, (c) with gridless local search on the MAP function.

the error performance is evaluated, the two equivalent MISDP reformulations (20) and (22) are chosen according to the discussion in Section IV to achieve a lower computation time.

A. Uncorrelated Source Signals

We first compare the performance of the methods in the case with uncorrelated source signals that satisfy the prior assumption in (7). Specifically, for each Monte-Carlo trial, the true source signals in Ψ are randomly generated according to the uncorrelated Gaussian prior in (7) with the variance $\gamma = 1$.

In the simulations in Fig. 2 and 3, we compare the estimation error performance of the different methods in a small-scale scenario of $L = 3$ sources with spatial frequencies $\mu = \pi \cdot [-0.1, 0.35, 0.5]^T$, where the brute-force search is

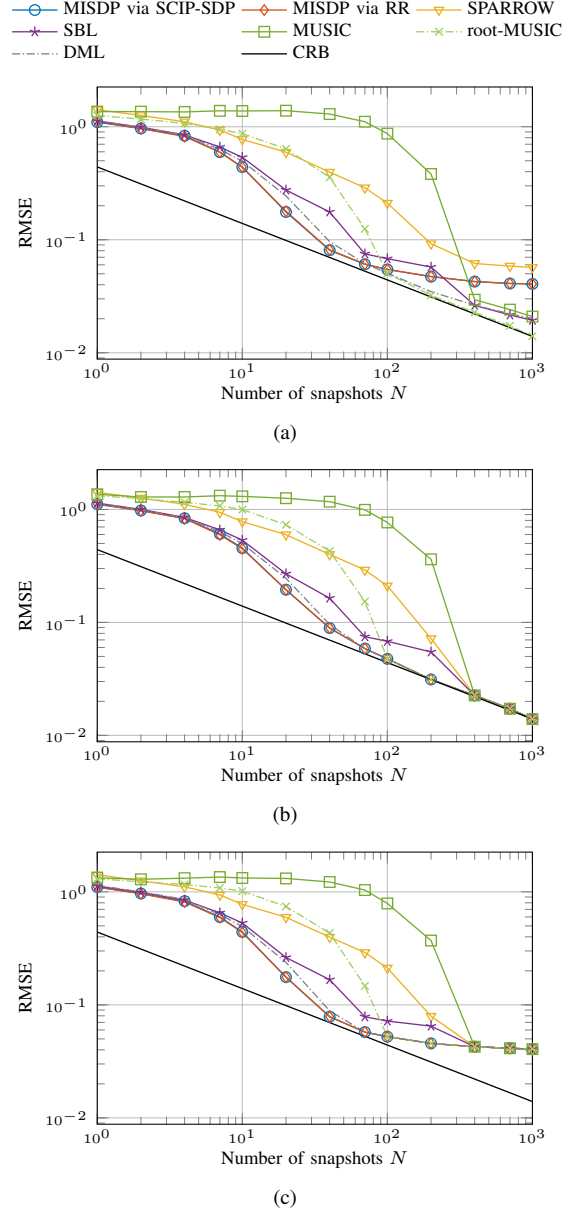


Fig. 3. Error performance w.r.t. the number of snapshots for $L = 3$ uncorrelated sources, $M = 8$ sensors, $\text{SNR} = -5$ dB, and $K = 100$ grid points, in the case (a) without gridless local search, (b) with gridless local search on the DML function, (c) with gridless local search on the MAP function.

computationally competitive. The true frequencies μ are not forced to be on the searching grid. The estimation errors of the recovered frequencies without and with the additional gridless local search based on the DML function and the MAP function in (17), respectively, are reported.

In the first simulation, as depicted in Fig. 2, the number of snapshots is set to be $N = 8$ and the SNR is varied between -10 dB and 20 dB. Except for root-MUSIC, all the methods are grid-based and, hence, as shown in Fig. 2(a), their estimation quality in the high SNR region is hindered by the grid mismatch error caused by the finite grid. Nevertheless, in most of the cases, the grid mismatch error can be eliminated by an additional gridless local search, as demonstrated in Fig. 2(b)

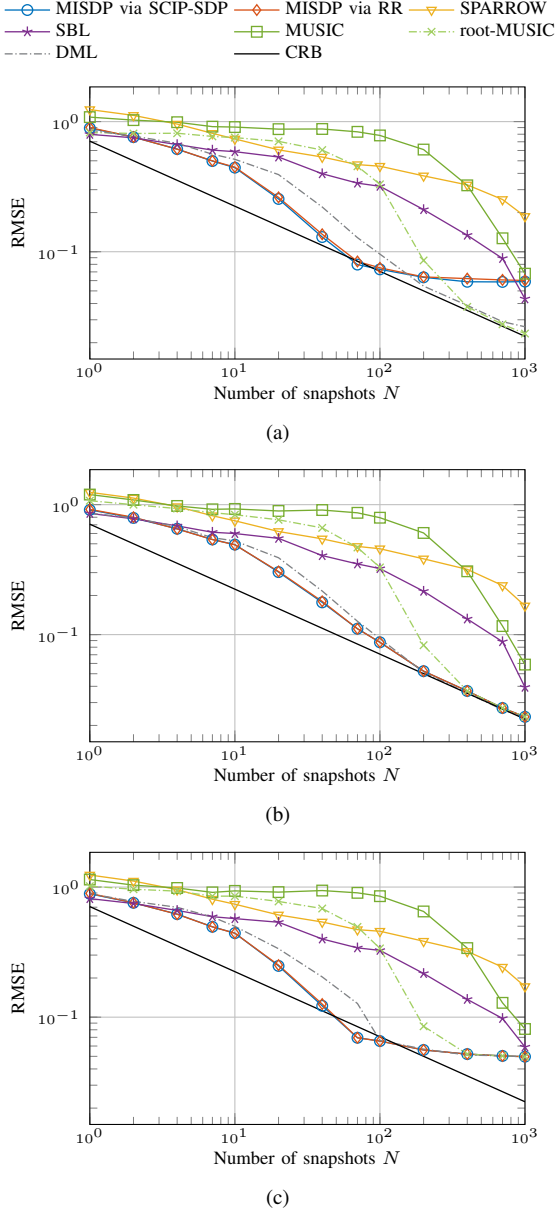


Fig. 4. Error performance w.r.t. the number of snapshots for $L = 5$ uncorrelated sources, $M = 8$ sensors, $\text{SNR} = -5$ dB, and $K = 100$ grid points, in the case (a) without gridless local search, (b) with gridless local search on the DML function, (c) with gridless local search on the MAP function.

and 2(c). With the increase of SNR, the solution of SPARROW becomes less sparse than the expected value since the recommended choice of the regularization parameter λ in (32) decreases. This results in a significant degradation of the error performance of SPARROW in the high SNR region. A more suitable choice of λ may be obtained by cross validation with training data, which is, however, not investigated in this paper. Compared to SCIP-SDP, the randomized rounding algorithm is capable of obtaining a satisfactory approximate solution of the proposed MISDP problem (20) or (22). The proposed MISDP-based method, the brute-force DML, and the SBL method exhibit comparable SNR thresholds at which their RMSEs achieve the CRB. These thresholds are superior to those of

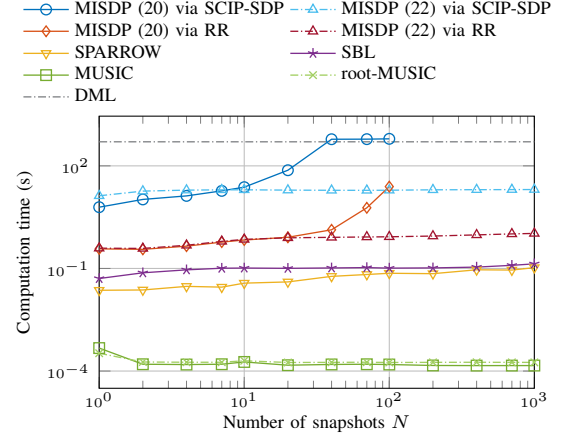


Fig. 5. Computation time vs. the number of snapshots for $L = 5$ uncorrelated sources, $M = 8$ sensors, $\text{SNR} = -5$ dB, and $K = 100$ grid points.

the other methods examined. Moreover, the proposed method also exhibits the best estimation quality in the region before the threshold.

In the second simulation, as shown in Fig. 3, the SNR is fixed at -5 dB and the number of snapshots is varied from 1 to 10^3 . Similar to Fig. 2, Fig. 3 demonstrates that the randomized rounding algorithm finds a satisfactory approximate solution of the MISDP problem (20) or (22) in the inspected sample size region, as compared to the exact solution obtained by SCIP-SDP. As shown in Fig. 3(a), due to the continuous relaxation and the Lagrangian relaxation discussed in Section VI, SPARROW is outperformed by the brute-force DML and the proposed method in both the asymptotic and non-asymptotic regions. The brute-force DML and the proposed method exhibit the best threshold performance. As mentioned in Section III, the MAP estimation problem differs from the DML only in the additional Tikhonov regularization introduced by the Gaussian prior. Compared to the unbiased DML estimator, the use of additional knowledge of the waveform's prior distribution in the MAP estimator, when it is consistent with the true prior, typically leads to decreased estimation variance but increased bias, which is rooted in the well-known bias-variance trade-off [59, Sec. 6.2]. As a result revealed in Fig. 3(a), the proposed MAP-based method possesses a lower estimation error than DML in the region of low sample sizes but, for large sample sizes, the RMSE of the proposed method is dominated by the asymptotic bias. Nevertheless, as shown in Fig. 3(b), the proposed method can still be used to obtain a good initialization for the gridless local search on the DML function in the asymptotic region. Different from the results in Fig. 2, the threshold of SBL occurs at a higher number of snapshots than that of DML. In addition, for all the compared methods, both the bias introduced by the regularization terms and the residual error caused by the finite grid can be eliminated in the asymptotic region by the additional gridless local search on the DML function.

Next, we consider a scenario of $L = 5$ sources with frequencies $\mu = \pi \cdot [-0.5, 0.1, 0.35, 0.5, 0.7]^T$, which becomes more difficult as the number of feasible binary solutions for prob-

lem (20) increases exponentially with increasing L . Hence, we increase the number T of randomly generated binary solutions to 10^5 for the randomized rounding Algorithm 1. Moreover, the solution obtained by Algorithm 1 is chosen to be the initialization for SCIP-SDP, which provides a better initial upper bound of the optimal value and, consequently, accelerates the branch-and-bound process in SCIP-SDP.² The estimation error performance is reported in Fig. 4 and the computation time in Fig. 5. The complexities of the two equivalent MISDP reformulations (20) and (22) are compared when solved by the SCIP-SDP solver and the randomized rounding Algorithm 1. Due to the high computation time of the brute-force DML, the results are averaged over only $N_R = 200$ Monte-Carlo trials. The computation time of the additional gridless local search by `fmincon` is negligible compared to SPARROW and, hence, is not reported. Although the branch-and-bound strategy employed by SCIP-SDP enjoys improved scalability compared to the brute-force search, to limit the total execution time of this simulation, we terminate the SCIP-SDP solver when 500 branch-and-bound nodes have been explored or a time limit of 600 seconds has been achieved. Compared to the simulation in Fig. 3, two major differences are observed in Fig. 4. First, as mentioned in Section V, due to the incorporation of a randomized rounding procedure in the branch-and-bound approach, the SCIP-SDP solver often quickly finds a nearly optimal solution but spends much more time improving the lower bounds to verify the optimality of the obtained solution. Therefore, although only 500 branch-and-bound nodes have been visited, the proposed method via SCIP-SDP presents a more significant decrease of the RMSE compared to DML in the region of a low sample size than that in Fig. 3, which also leads to a threshold performance superior to DML. In fact, even without the branch-and-bound, the randomized rounding Algorithm 1 already finds a solution of similar estimation quality for a proper choice of T . This suggests that, for a low sample size, our proposed MISDP-based method with the randomized rounding algorithm is more favorable than the brute-force DML since it possesses not only a superior error performance but also a reduced running time, as shown in Fig. 5. Second, all the other methods, except for the DML and the proposed MISDP-based method, exhibit a degradation of error performance. Moreover, since the MAP estimation model incorporates the additional prior information of the source covariance matrix, which is assumed to be unknown in the stochastic model for the CRB, the proposed method via SCIP-SDP achieves an RMSE below the CRB in Fig. 4(c) in the middle region.

We then analyze the computation time of the two equivalent MISDP reformulations (20) and (22) for the sparse MAP estimation problem presented in Fig. 5. The problems (20) and (22) differ only in the semidefinite constraint, in particular, in their dimensions. The computation time of an interior-point solver for continuous SDP problems generally increases dramatically with the increase of the dimensions of the

semidefinite constraints. In particular, for both the randomized rounding Algorithm 1 and the SCIP-SDP solver, the difference in the dimension of the semidefinite constraints between the formulations (20) and (22) only affects the computation time of the relaxed continuous SDP problem or subproblems in the branch-and-bound process, whereas the randomized rounding step in Algorithm 1 and the searching path over the branch-and-bound tree are independent of the choice of the MISDP formulation. In contrast to the semidefinite constraint (20b), the dimension of the constraint (22b) becomes independent of the number of snapshots N by introducing an equivalent reformulated data matrix with $N = M$. Therefore, consistent with the above theoretical analysis, in Fig. 5, the computation time of SCIP-SDP and the randomized rounding Algorithm 1 for the MISDP formulation (20) increases exponentially with the increase of the number of snapshots, whereas the computation time remains constant when the formulation (22) is used. However, considering the computation time of the randomized rounding step in Algorithm 1, there is no significant difference in the total computation time of Algorithm 1 between the two formulations in the undersampled region. Note that, a time limit of 600 seconds is set for the SCIP-SDP solver and the formulation (20) is only considered for a sample size up to 100 due to high computation time.

B. Correlated Source Signals

We then evaluate the performance of the methods in the case with correlated source signals. In particular, we consider $L = 3$ sources with frequencies $\boldsymbol{\mu} = \pi \cdot [-0.1, 0.35, 0.5]^T$. The source signals follow a zero-mean complex Gaussian distribution with the covariance matrix

$$\begin{bmatrix} 1 & \varphi & \varphi^2 \\ \varphi^* & 1 & \varphi^2 \\ \varphi^* & \varphi^{*2} & 1 \end{bmatrix} \quad (33)$$

and the correlation coefficient $\varphi \in \mathbb{C}$ between source 1 and 2 is chosen to be $\varphi = 0.99$. Since all sources are set to have the same average power of 1, the regularization ρ in our proposed method is still chosen according to the rule in (9) with $P_\Psi = 1$. The estimation errors for various choices of the number of snapshots are displayed in Fig. 6. The following differences can be observed compared to the results in Fig. 3 for uncorrelated sources. First, it is verified that the subspace-based methods, including MUSIC and root-MUSIC, often fail for correlated sources. On the other hand, the SBL method exhibits a significant degradation of the error performance due to the mismatch of the prior model. Although the RMSE of the brute-force DML and the proposed method also increases in the post-threshold region, the increase in RMSE is insignificant.

IX. CONCLUSION

In this paper, we consider the maximum a posteriori (MAP) estimation for joint sparse signal reconstruction from multiple measurement vectors (MMV) with application to DOA estimation, which is conventionally formulated as a regularized least-squares (LS) problem with $\ell_{2,0}$ -norm constraint. Using

²One may alternatively increase the number of randomly generated binary solutions in the internal randomized rounding procedure in SCIP-SDP, which is, however, impossible with the current version of the MATLAB interface of the SCIP-SDP solver.

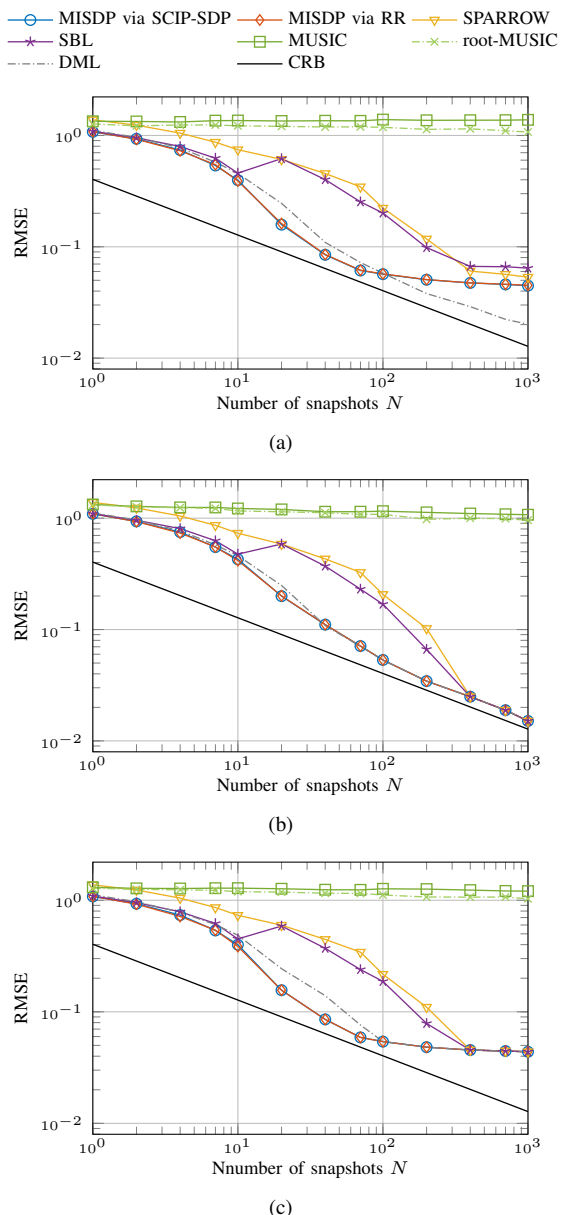


Fig. 6. Error performance w.r.t. the number of snapshots for $L = 3$ correlated sources, $M = 8$ sensors, $\text{SNR} = -5$ dB, and $K = 100$ grid points, in the case (a) without gridless local search, (b) with gridless local search on the DML function, (c) with gridless local search on the MAP function.

the reformulation techniques in [14], [39], we reformulate the $\ell_{2,0}$ -norm constrained LS problem exactly as a mixed-integer semidefinite program (MISDP). By doing so, a provably global optimal solution of the sparse MAP estimation problem can be obtained by an efficient MISDP solver based on the state-of-the-art branch-and-bound method, such as SCIP-SDP [40]–[42]. One attractive feature of this approach is that, if the branch-and-bound solver is terminated early, an optimality assessment of the obtained solution is provided by the gap between the lower and upper bounds of the optimal value. However, we remark that the branch-and-bound gap does not necessarily reflect the estimation quality of the solution since even the global optimal solution of the MAP estimation problem may possess an estimation bias. Due to the incorporation

of a randomized rounding procedure in the branch-and-bound approach, the SCIP-SDP solver often quickly finds an optimal or nearly optimal solution, but the verification of the optimality of the obtained solution may become computationally expensive for problems of extremely large dimensions. Motivated by the above observation, we alternatively apply a randomized rounding algorithm, similar to the algorithm proposed by Pilanci et al. in [39] for the MISDP reformulation in the case with a single measurement, directly to the proposed MISDP reformulation in order to obtain a satisfactory approximate solution at a further reduced computation time in the case of large problem dimensions. Numerical simulations demonstrate the improved error performance of our proposed method in comparison to several widely used DOA estimation methods. In particular, compared to the deterministic maximum likelihood (DML) estimator obtained by the brute-force search, the proposed MISDP-based method with the randomized rounding algorithm exhibits a superior error performance at a considerably reduced running time in difficult scenarios, e.g., the case with a limited number of snapshots. Also, similar to the DML estimator, the proposed method provides an improved robustness to the source correlations and the increase of the number of sources when compared to subspace-based methods and the SBL method. Similar to our proposed method, the sparse Bayesian learning (SBL) method adopts an uncorrelated Gaussian prior assumption. However, instead of considering the source variances as tuning parameters, it estimates the source variances by a type-II maximum likelihood approach. Although the SBL method provides more flexibility and avoids the overhead of tuning regularization parameters, it shows a significant degradation of the error performance in the simulation with correlated sources due to the mismatch of the prior model. Additionally, in contrast to other nonconvex approaches, including the greedy methods and the SBL method, the proposed MISDP-based method can find a provably global optimal solution via a branch-and-bound solver.

REFERENCES

- [1] I. F. Gorodnitsky, J. S. George, and B. D. Rao, “Neuromagnetic source imaging with FOCUSS: a recursive weighted minimum norm algorithm,” *Electroencephalography and Clinical Neurophysiology*, vol. 95, no. 4, pp. 231–251, Oct. 1995.
- [2] I. Fevrier, S. Gelfand, and M. Fitz, “Reduced complexity decision feedback equalization for multipath channels with large delay spreads,” *IEEE Trans. Commun.*, vol. 47, no. 6, pp. 927–937, Jun. 1999.
- [3] S. Cotter, B. Rao, K. Engan, and K. Kreutz-Delgado, “Sparse solutions to linear inverse problems with multiple measurement vectors,” *IEEE Trans. Signal Process.*, vol. 53, no. 7, pp. 2477–2488, Jul. 2005.
- [4] P. Stoica and R. L. Moses, *Spectral analysis of signals*. Upper Saddle River, N.J.: Pearson/Prentice Hall, 2005.
- [5] W. Dong, G. Shi, Y. Ma, and X. Li, “Image restoration via simultaneous sparse coding: where structured sparsity meets Gaussian scale mixture,” *Int J Comput Vis*, vol. 114, no. 2, pp. 217–232, Sep. 2015.
- [6] X. Zheng, X. Sun, K. Fu, and H. Wang, “Automatic annotation of satellite images via multifeature joint sparse coding with spatial relation constraint,” *IEEE Geosci. Remote Sens. Lett.*, vol. 10, no. 4, pp. 652–656, Jul. 2013.
- [7] J. A. Tropp, “Algorithms for simultaneous sparse approximation. Part II: Convex relaxation,” *Signal Processing*, vol. 86, no. 3, pp. 589–602, Mar. 2006.
- [8] J. A. Tropp, A. C. Gilbert, and M. J. Strauss, “Algorithms for simultaneous sparse approximation. Part I: Greedy pursuit,” *Signal Processing*, vol. 86, no. 3, pp. 572–588, Mar. 2006.

- [9] B. K. Natarajan, "Sparse approximate solutions to linear systems," *SIAM J. Comput.*, vol. 24, no. 2, pp. 227–234, Apr. 1995.
- [10] G. Davis, S. Mallat, and M. Avellaneda, "Adaptive greedy approximations," *Constr. Approx.*, vol. 13, no. 1, pp. 57–98, Mar. 1997.
- [11] D. Needell and J. A. Tropp, "CoSaMP: iterative signal recovery from incomplete and inaccurate samples," *Applied and Computational Harmonic Analysis*, vol. 26, no. 3, pp. 301–321, May 2009.
- [12] M. E. Davies and Y. C. Eldar, "Rank awareness in joint sparse recovery," *IEEE Trans. Inf. Theory*, vol. 58, no. 2, pp. 1135–1146, Feb. 2012.
- [13] D. Malioutov, M. Cetin, and A. Willsky, "A sparse signal reconstruction perspective for source localization with sensor arrays," *IEEE Trans. Signal Process.*, vol. 53, no. 8, pp. 3010–3022, Aug. 2005.
- [14] C. Steffens, M. Pesavento, and M. E. Pfetsch, "A compact formulation for the $\ell_{2,1}$ mixed-norm minimization problem," *IEEE Trans. Signal Process.*, vol. 66, no. 6, pp. 1483–1497, Mar. 2018.
- [15] M. Kowalski, "Sparse regression using mixed norms," *Applied and Computational Harmonic Analysis*, vol. 27, no. 3, pp. 303–324, Nov. 2009.
- [16] D. P. Wipf and B. D. Rao, "An empirical Bayesian strategy for solving the simultaneous sparse approximation problem," *IEEE Trans. Signal Process.*, vol. 55, no. 7, pp. 3704–3716, Jul. 2007.
- [17] P. Gerstoft, C. F. Mecklenbräuker, A. Xenaki, and S. Nannuru, "Multisnapshot sparse Bayesian learning for DOA," *IEEE Signal Process. Lett.*, vol. 23, no. 10, pp. 1469–1473, Oct. 2016.
- [18] S. S. Chen, D. L. Donoho, and M. A. Saunders, "Atomic decomposition by basis pursuit," *SIAM Rev.*, vol. 43, no. 1, pp. 129–159, Jan. 2001.
- [19] R. Tibshirani, "Regression shrinkage and selection via the lasso," *R. Stat. Soc.*, vol. 58, no. 1, pp. 267–288, 1996.
- [20] R. Gribonval, "Should penalized least squares regression be interpreted as maximum a posteriori estimation?" *IEEE Trans. Signal Process.*, vol. 59, no. 5, pp. 2405–2410, May 2011.
- [21] Y. Jin and B. D. Rao, "Support recovery of sparse signals in the presence of multiple measurement vectors," *IEEE Trans. Inf. Theory*, vol. 59, no. 5, pp. 3139–3157, May 2013.
- [22] J. Chen and X. Huo, "Theoretical results on sparse representations of multiple-measurement vectors," *IEEE Trans. Signal Process.*, vol. 54, no. 12, pp. 4634–4643, Dec. 2006.
- [23] M.-J. Lai and Y. Liu, "The null space property for sparse recovery from multiple measurement vectors," *Applied and Computational Harmonic Analysis*, vol. 30, no. 3, pp. 402–406, May 2011.
- [24] L. Ramesh, C. R. Murthy, and H. Tyagi, "Sample-measurement tradeoff in support recovery under a subgaussian prior," *IEEE Trans. Inf. Theory*, vol. 67, no. 12, pp. 8140–8153, Dec. 2021.
- [25] S. Khanna and C. R. Murthy, "On the support recovery of jointly sparse gaussian sources via sparse bayesian learning," *IEEE Trans. Inf. Theory*, vol. 68, no. 11, pp. 7361–7378, Nov. 2022.
- [26] H. Krim and M. Viberg, "Two decades of array signal processing research: the parametric approach," *IEEE Signal Process. Mag.*, vol. 13, no. 4, pp. 67–94, Jul. 1996.
- [27] H. L. Van Trees, *Optimum array processing*. New York, USA: John Wiley & Sons, Inc., Mar. 2002.
- [28] A. M. Zoubir, M. Viberg, R. Chellappa, and S. Theodoridis, Eds., *Array and statistical signal processing*, first edition ed., ser. Academic Press library in signal processing. Amsterdam: Academic Press, 2014, no. v. 3.
- [29] M. Pesavento, M. Trinh-Hoang, and M. Viberg, "Three more decades in array signal processing research: an optimization and structure exploitation perspective," *IEEE Signal Process. Mag.*, vol. 40, no. 4, pp. 92–106, Jun. 2023.
- [30] W. Liu, M. Haardt, M. S. Greco, C. F. Mecklenbräuker, and P. Willett, "Twenty-five years of sensor array and multichannel signal processing: a review of progress to date and potential research directions," *IEEE Signal Process. Mag.*, vol. 40, no. 4, pp. 80–91, Jun. 2023.
- [31] R. Schmidt, "Multiple emitter location and signal parameter estimation," *IEEE Trans. Antennas Propag.*, vol. 34, no. 3, pp. 276–280, Mar. 1986.
- [32] A. Barabell, "Improving the resolution performance of eigenstructure-based direction-finding algorithms," in *ICASSP 83 IEEE Int. Conf. Acoust. Speech Signal Process.*, vol. 8, Apr. 1983, pp. 336–339.
- [33] R. Roy and T. Kailath, "ESPRIT-estimation of signal parameters via rotational invariance techniques," *IEEE Trans. Acoust. Speech Signal Process.*, vol. 37, no. 7, pp. 984–995, Jul. 1989.
- [34] M. Haardt and J. A. Nosske, "Unitary ESPRIT: how to obtain increased estimation accuracy with a reduced computational burden," *IEEE Trans. Signal Process.*, vol. 43, no. 5, pp. 1232–1242, May 1995.
- [35] Y. C. Eldar and G. Kutyniok, Eds., *Compressed sensing: theory and applications*. Cambridge ; New York: Cambridge University Press, 2012.
- [36] Z. Yang, J. Li, P. Stoica, and L. Xie, "Sparse methods for direction-of-arrival estimation," in *Academic Press Library in Signal Processing, Volume 7*, R. Chellappa and S. Theodoridis, Eds. Academic Press, Jan. 2018, pp. 509–581.
- [37] P. Gerstoft and C. F. Mecklenbräuker, "Wideband sparse bayesian learning for DOA estimation from multiple snapshots," in *2016 IEEE Sens. Array Multichannel Signal Process. Workshop SAM*, Jul. 2016, pp. 1–5.
- [38] P. Gerstoft, S. Nannuru, C. F. Mecklenbräuker, and G. Leus, "DOA estimation in heteroscedastic noise with sparse Bayesian learning," in *2018 IEEE Int. Conf. Acoust. Speech Signal Process. ICASSP*, Apr. 2018, pp. 3459–3463.
- [39] M. Pilić, M. J. Wainwright, and L. El Ghaoui, "Sparse learning via Boolean relaxations," *Math. Program.*, vol. 151, no. 1, pp. 63–87, Jun. 2015.
- [40] T. Gally, M. E. Pfetsch, and S. Ulbrich, "A framework for solving mixed-integer semidefinite programs," *Optim. Methods Softw.*, vol. 33, no. 3, pp. 594–632, May 2018.
- [41] F. Matter and M. E. Pfetsch, "Presolving for mixed-integer semidefinite optimization," *INFORMS J. Optim.*, vol. 5, no. 2, pp. 131–154, Apr. 2023.
- [42] C. Hojny and M. E. Pfetsch, "Handling symmetries in mixed-integer semidefinite programs," in *Integr. Constraint Program. Artif. Intell. Oper. Res.*, A. A. Cire, Ed., vol. 13884. Cham: Springer Nature Switzerland, 2023, pp. 69–78.
- [43] S. Boyd and L. Vandenberghe, *Convex optimization*. Cambridge University Press, 2004.
- [44] V. Monga, Y. Li, and Y. C. Eldar, "Algorithm unrolling: interpretable, efficient deep learning for signal and image processing," *IEEE Signal Process. Mag.*, vol. 38, no. 2, pp. 18–44, Mar. 2021.
- [45] L. Vandenberghe and S. Boyd, "Semidefinite programming," *SIAM Rev.*, vol. 38, no. 1, pp. 49–95, Mar. 1996.
- [46] MOSEK ApS, "The MOSEK optimization toolbox for MATLAB. Version 10.0.38." <https://docs.mosek.com/latest/toolbox/index.html>, 2023.
- [47] M. Schmidt, E. Berg, M. Friedlander, and K. Murphy, "Optimizing costly functions with simple constraints: a limited-memory projected quasi-Newton algorithm," in *Proc. Twelfth Int. Conf. Artif. Intell. Stat.* PMLR, Apr. 2009, pp. 456–463.
- [48] S. Boyd, N. Parikh, E. Chu, B. Peleato, and J. Eckstein, "Distributed optimization and statistical learning via the alternating direction method of multipliers," *Found. Trends® Mach. Learn.*, vol. 3, no. 1, pp. 1–122, 2011.
- [49] P. Raghavan and C. D. Tompson, "Randomized rounding: a technique for provably good algorithms and algorithmic proofs," *Combinatorica*, vol. 7, no. 4, pp. 365–374, Dec. 1987.
- [50] R. Motwani and P. Raghavan, *Randomized algorithms*. Cambridge: Cambridge University Press, 1995.
- [51] D. P. Williamson and D. B. Shmoys, *The design of approximation algorithms*. Cambridge: Cambridge University Press, 2011.
- [52] Y. Chi, L. L. Scharf, A. Pezeshki, and A. R. Calderbank, "Sensitivity to basis mismatch in compressed sensing," *IEEE Trans. Signal Process.*, vol. 59, no. 5, pp. 2182–2195, May 2011.
- [53] M. A. Herman and T. Strohmer, "General deviants: an analysis of perturbations in compressed sensing," *IEEE J. Sel. Top. Signal Process.*, vol. 4, no. 2, pp. 342–349, Apr. 2010.
- [54] I. Ziskind and M. Wax, "Maximum likelihood localization of multiple sources by alternating projection," *IEEE Trans. Acoust. Speech Signal Process.*, vol. 36, no. 10, pp. 1553–1560, Oct. 1988.
- [55] M. C. Grant and S. P. Boyd, "CVX: matlab software for disciplined convex programming, version 2.2," <http://cvxr.com/cvx/>, Jan. 2020.
- [56] —, "Graph implementations for nonsmooth convex programs," in *Recent Adv. Learn. Control*, ser. Lecture Notes in Control and Information Sciences, V. D. Blondel, S. P. Boyd, and H. Kimura, Eds. London: Springer, 2008, pp. 95–110.
- [57] P. Stoica, E. G. Larsson, and A. B. Gershman, "The stochastic CRB for array processing: a textbook derivation," *IEEE Signal Process. Lett.*, vol. 8, no. 5, pp. 148–150, May 2001.
- [58] B. N. Bhaskar, G. Tang, and B. Recht, "Atomic norm denoising with applications to line spectral estimation," *IEEE Trans. Signal Process.*, vol. 61, no. 23, pp. 5987–5999, Dec. 2013.
- [59] G. James, D. Witten, T. Hastie, and R. Tibshirani, *An introduction to statistical learning: with applications in R*, ser. Springer Texts in Statistics. New York, NY: Springer US, 2021.